Clim Dyn (2012) 38:595–611
DOI 10.1007/s00382-011-1183-1

Modeling the hydroclimatology of the midwestern United States. Part 2: future climate

Jonathan M. Winter · Elfatih A. B. Eltahir

Received: 3 August 2010 / Accepted: 30 August 2011 / Published online: 15 September 2011

Abstract An ensemble of six 22-year numerical experiments was conducted to quantify the response of soil moisture to multiple climate change scenarios over the American Midwest. Regional Climate Model version 3 (RegCM3) was run using two surface physics schemes: Integrated Biosphere Simulator (IBIS) and Biosphere-Atmosphere Transfer Scheme 1e (BATS1e); and two convective closure assumptions: Fritsch and Chappell and Arakawa and Schubert. Experiments were forced with a surrogate climate change scenario constructed using the National Centers for Environmental Prediction-Department of Energy Reanalysis 2 dataset and the ECHAM5 A1B climate change scenario. RegCM3-IBIS and RegCM3-BATS1e simulate increased two-meter air temperature and downward longwave radiation throughout the year under both climate change scenarios. While differences in shortwave radiation are relatively small; some model configurations and climate change scenarios produce additional precipitation, evapotranspiration, and total runoff during the spring and summer. Soil moisture is unchanged or increased throughout the growing season as enhanced rainfall offsets greater evaporative demand. Negligible drying in root zone soil moisture is found in all climate change experiments conducted, regardless of surface physics scheme, boundary conditions, or convective closure assumption.

J. M. Winter (✉) · E. A. B. Eltahir
Massachusetts Institute of Technology, Cambridge, MA, USA
e-mail: jwinter@mit.edu; jwinter@giss.nasa.gov

Present Address:
J. M. Winter
NASA Goddard Institute for Space Studies,
New York, NY, USA

Keywords Hydrology · Regional climate modeling · Climate change · Soil moisture · Midwestern United States

1 Introduction

In 1988, a severe drought during the spring and summer reduced crop yields in the United States by approximately 37%, prompting a $3-billion Congressional bailout for farmers (Rosenzweig et al. 2001). Agricultural productivity is strongly correlated with soil moisture, and as the world's food supply continues to be taxed by population growth and rapidly developing economies, a greater percentage of arable land will need to be utilized and land currently producing food must become more efficient (Harrison et al. 2002).

Climate change is likely to accelerate the hydrologic cycle, leading to enhanced global precipitation and evapotranspiration. In areas where the increase in evapotranspiration significantly exceeds that of precipitation, drought conditions will become more common. This could have extensive impacts on the entire world community if the newly created droughts occur in the midwestern United States or southern Europe, regions of substantial agricultural productivity. However, if the increase in precipitation exceeds that of evapotranspiration, little or no drying will occur. Fig. 1 shows two potential responses of soil moisture to climate change. The left panel depicts soil drying, where reduced precipitation coupled with significantly enhanced latent heat flux decreases soil moisture. The right panel shows unchanged soil moisture. Here, additional precipitation, modest latent heat flux increases resulting from strong controls on evapotranspiration by plants, and greater total runoff balance to have a minimal effect on soil moisture. Note that the terms "latent heat flux" and

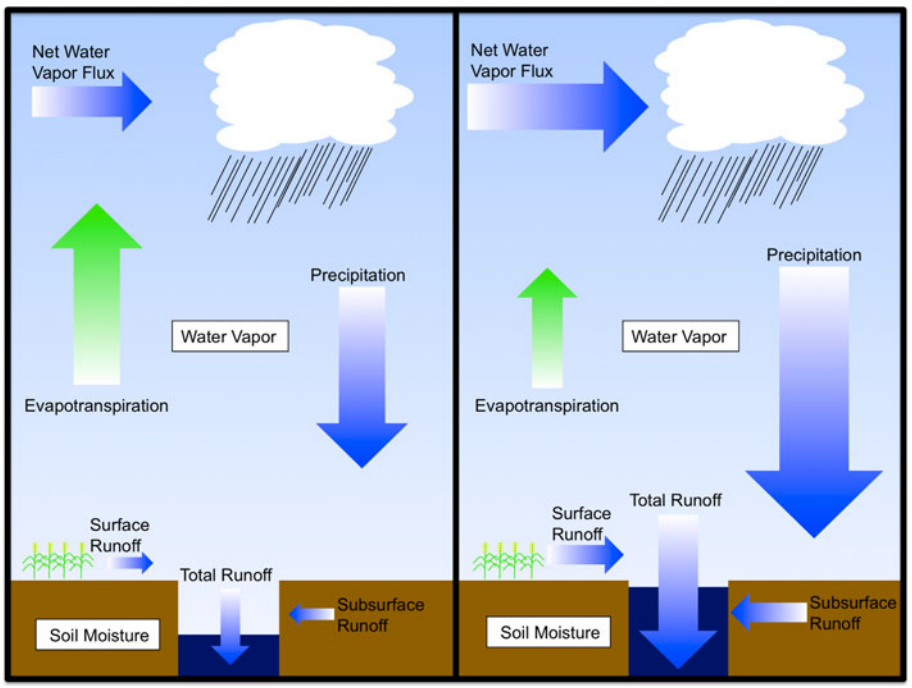

Fig. 1 Mechanisms for soil drying (*left*) and unchanged soil moisture (*right*)

"evapotranspiration" are used interchangeably throughout this paper.

One of the first analyses of the response of soil moisture to climate change was completed by Manabe et al. in (1981). Using the NOAA Geophysical Fluid Dynamics Laboratory (GFDL) general circulation model (GCM) with three different arrangements of topography and resolution, Manabe et al. (1981) found soil moisture reductions in middle and high latitudes during the summer. Recently, in more detailed studies, Manabe and Wetherald (2002) and Manabe et al. (2004) concluded that the American Midwest experiences summer drying and winter wetting under the Intergovernmental Panel on Climate Change IS92a scenario and a 4 × CO_2 scenario. In the winter, rainfall is enhanced by increased moisture transport from warmer oceans and cold surface temperatures cause the additional available energy produced by climate change to be partitioned into sensible heat (Manabe et al. 2004). In contrast, during the summer surface temperatures are warmer and latent heat flux is enhanced, outpacing any increase in precipitation from the oceans, thus drying the soils.

Summer soil moisture drying over the American Midwest was also found by Wang (2005) and Diffenbaugh and Ashfaq (2010). Wang (2005) conducted a comprehensive study on the potential for future drought using fifteen different GCMs. The majority of models examined simulated extensive summer drying and some winter wetting over mid-latitude North America. Diffenbaugh and Ashfaq (2010) used an ensemble of five Regional Climate Model version 3 (RegCM3) simulations forced with a climate change scenario (2030–2039) derived from the National Center for Atmospheric Research (NCAR) Community Climate System Model 3 to show that future precipitation, evapotranspiration, and soil moisture all decrease.

However, this trend is not found in all studies. A comparison of the GFDL and NCAR GCMs forced using a 2 × CO_2 climate change scenario concluded that land surface parameterizations play a pivotal role in the study of summer dryness (Meehl and Washington 1988). In these simulations, the GFDL model retained less of the precipitation increase of the winter months than the NCAR GCM, partitioning it to runoff as opposed to groundwater recharge, making the GFDL model drier during the spring and summer. In contrast, water added throughout the winter and early spring to the NCAR model reduced and sometimes eliminated summer drying. Seneviratne et al. (2002) concluded that decreases in soil moisture over the midwestern United States were weak compared to the warming forcing applied, on the order of 1 to 2% of saturation, using a series of RegCM3 experiments. They hypothesized that vegetative controls on transpiration and enhanced infiltration during the spring mitigate summer drying. The deviation of these results from those of Manabe et al. (1981) was explained through a series of experiments illustrating the differences between the land surface parameterizations used in the two studies.

Recently, the U.S. Global Change Research Program released a comprehensive report detailing the impacts of climate change on the United States. Karl et al. (2009) concluded that agriculture in the midwestern United States is likely to benefit from low levels of warming, a result of a longer growing season and CO_2 fertilization. However,

larger changes in temperature and precipitation associated with higher levels of warming will be detrimental to crop growth and yields. In addition, more intense rainfall during the summer is likely to result in longer periods of time between precipitation events, which coupled with enhanced evapotranspiration will increase the likelihood of drought (Karl et al. 2009; Wuebbles and Hayhoe 2004).

Disparate findings of previous studies suggest that choice of model, model configuration, and warming forcing applied substantially influence results. To quantify the local response of soil moisture in the midwestern United States to future climate across model configurations and warming forcings, a series of Regional Climate Model version 3 (RegCM3) simulations using multiple surface physics schemes and convective closure assumptions driven with boundary conditions from two future climate scenarios was run. Context for the assessment of climate change over the American Midwest presented below is provided by a thorough comparison of RegCM3 coupled to both Integrated Biosphere Simulator (IBIS) and Biosphere-Atmosphere Transfer Scheme 1e (BATS1e), described in the companion paper.

2 Model description and development

Relevant model definitions and citations for Regional Climate Model version 3 (RegCM3), Biosphere-Atmosphere Transfer Scheme 1e (BATS1e), Integrated Biosphere Simulator (IBIS), and the Grell convective scheme are included in this section. A more detailed description of each model is provided in the companion paper.

RegCM3 is a 3-dimensional, sigma-coordinate, hydrostatic, compressible regional climate model (Pal et al. 2007). BATS1e is a comprehensive model of land surface processes that can be run offline, coupled to a GCM, or coupled to RegCM3 (Dickinson et al. 1993). IBIS is a surface physics scheme developed by Foley et al. (1996) at the University of Wisconsin-Madison. The coupling of IBIS to RegCM3 is described in Winter et al. (2009). The Grell scheme is a basic representation of convective precipitation similar in structure to the Arakawa & Schubert scheme (Arakawa and Schubert 1974), and can be closed using two assumptions: the Arakawa & Schubert closure (AS74) (Grell et al. 1994) and the Fritsch & Chappell closure (FC80) (Fritsch and Chappell 1980).

3 Design of experiments

All climate change experiments are identical in domain to the control experiments described in the companion paper. Simulations are centered at 40°N, 95°W and use a Rotated Mercator projection. The domain covers all of the United States, as well as parts of Mexico and Canada (Fig. 2), spanning 100 points zonally, 60 points meridionally at a horizontal grid spacing of 60 km. Simulations were allowed to spin-up for 21 months. The region evaluated is shown by the 4.0° × 5.5° shaded box contained in Fig. 2.

Initialization of vegetation, soil moisture, and soil temperature is identical to the control simulations and described in the companion paper. A brief review is provided below.

Vegetation classes in RegCM3-BATS1e were directly assigned using the USGS Global Land Cover Characterization (GLCC) dataset. In IBIS, each grid box was populated with plant functional types (PFTs) based on the potential global vegetation dataset of Ramankutty (1999) and two climate datasets. Croplands were then defined in RegCM3-IBIS using the USGS GLCC dataset. RegCM3-IBIS was run with static vegetation to create a consistent comparison between models. Topography for both models was given by the USGS Global 30-arc second elevation dataset (1996) aggregated to a 0.5° × 0.5° spatial resolution.

RegCM3-BATS1e initial soil moisture and soil temperature were set by the surface temperature boundary condition and vegetation type, respectively. Soil moisture, soil temperature, and soil ice were initialized in RegCM3-IBIS using an offline simulation of IBIS forced with monthly mean climatologies. Differences in the initialization of soil moisture and soil temperature were shown to be a relatively minor source of variability in the modeling results of similar experiments (Winter et al. 2009).

Two large-scale forcings were used to assess the response of soil moisture to future climate: a National

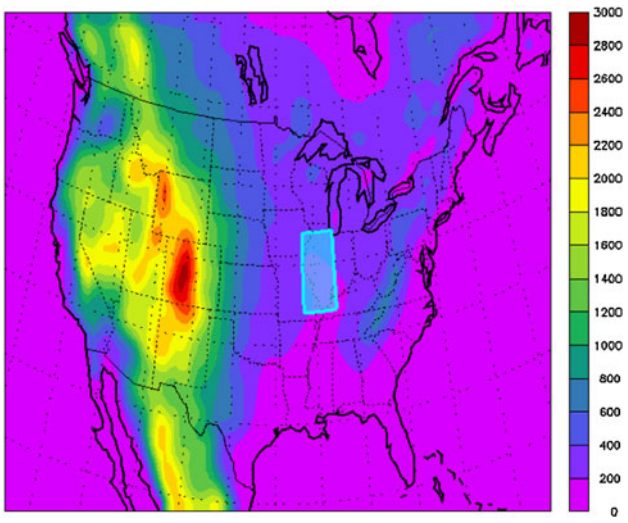

Fig. 2 Domain and topography (m) of climate change experiments with a 4.0° × 5.5° *cyan shaded box* delineating the extent of spatial averaging over American Midwest

Centers for Environmental Prediction (NCEP)-Department of Energy (DOE) Reanalysis 2 surrogate climate change scenario and the ECHAM5 GCM A1B climate change scenario.

3.1 NCEP-DOE Reanalysis 2 surrogate climate change

A surrogate climate change scenario was constructed based on the methodology of Schär et al. (1996) using the NCEP-DOE Reanalysis 2 (NNRP2) dataset. First, the boundaries were warmed by 3°C. Specifically, the NNRP2 dataset of temperature was increased by 3°C consistently throughout the atmospheric column, and sea surface temperatures derived from the National Oceanic and Atmospheric Administration (NOAA) Optimum Interpolation SST (OISST) dataset were warmed by 3°C. Relative humidity fields were left unchanged, resulting in an enhanced flux of water vapor at the boundaries. A global mean equilibrium surface temperature increase of 3°C corresponds approximately to a CO_2 equivalent concentration of 710 ppm (Randall et al. 2007). Therefore, the NNRP2 surrogate climate change simulations were run with a constant CO_2 concentration of 710 ppm, double the concentration of CO_2 (355 ppm) used in the NNRP2 control experiments. NNRP2 surrogate climate change experiments were initialized April 1st, 1982 and allowed to spin-up for 21 months. The subsequent 22 years (1984–2005) of simulated climate were assessed.

The surrogate climate change scenario described above is not a physically plausible representation of future climate. Constant warming throughout the atmospheric column and across the ocean is unrealistic. In addition, the matching of warmer atmospheric temperatures and CO_2 equivalent concentration is approximate, as increasing CO_2 equivalent concentration in the atmosphere will have varying regional effects on temperature. However, as a sensitivity analysis or crude representation of a warmer Earth, the surrogate climate change scenario has a number of advantages. First, boundary conditions are dynamically consistent with observed atmospheric flows (Schär et al. 1996). By basing the climate change scenario on reanalysis data, which integrates observations, regional climate models are guaranteed to be constrained by realistic atmospheric circulations. This is not true of GCM climate change simulations, which have complete freedom and could potentially introduce significant errors. Second, the procedure is model independent, and is therefore not subject to the biases of any particular GCM. And finally, surrogate climate change scenarios are intuitive and easy to implement (Schär et al. 1996).

To examine the model configuration variability of the NNRP2 surrogate climate change experiments, RegCM3-IBIS and RegCM3-BATS1e were run using the Grell parameterization of convection with the Fritsch & Chappell (FC80) and Arakawa & Schubert (AS74) convective closure assumptions. This produced an ensemble of four simulations: RegCM3-IBIS using AS74 (IBIS-AS), RegCM3-IBIS using FC80 (IBIS-FC), RegCM3-BATS1e using FC80 (BATS-FC), and RegCM3-BATS1e using AS74 (BATS-AS). Besides modified boundary conditions, SSTs, and an increased concentration of CO_2 equivalent; all other facets of the experimental design were identical to the NNRP2 control simulations, as described in the companion paper.

3.2 ECHAM5 GCM A1B

A climate change simulation of the ECHAM5 GCM (EH5OM) driven by the A1B emissions scenario of Nakicenovic et al. (2000) was used to force the boundaries and SSTs of RegCM3-IBIS and RegCM3-BATS1e. The concentration of CO_2 was increased over time as described by the A1B emissions scenario. EH5OM A1B climate change experiments were initialized April 1st, 2076 and allowed to spin-up for 21 months. The subsequent 22 years (2078–2099) of simulated climate were assessed.

While climate change boundary conditions generated by EH5OM are more complex to construct and vulnerable to errors specific to EH5OM, there are several advantages to using a GCM-driven climate change experiment. First, it allows for a more sophisticated representation of climate change. For example, the temperature of the entire atmospheric column will not uniformly warm by 3°C as described by the surrogate climate change scenario. Using a GCM allows for vertical differentiation in the temperature response. But more importantly, the GCM climate change scenario, unlike the surrogate climate change scenario, is not bound by current atmospheric flows. It is likely that climate change will significantly impact many aspects of the climate system at a variety of spatial scales. The EH5OM A1B scenario can include large-scale perturbations in atmospheric circulations resulting from climate change while the surrogate scenario cannot.

EH5OM A1B experiments were run using the configuration for convection in RegCM3-IBIS and RegCM3-BATS1e that best simulated the hydroclimatology of the American Midwest in the NNRP2 control experiments described in the companion paper: IBIS-AS and BATS-FC. Besides modified boundary conditions, SSTs, and an increased concentration of CO_2 equivalent, all other facets of the experimental design were identical to the EH5OM control simulations as described in the companion paper.

4 Results and discussion

Changes in the hydroclimatology of the American Midwest simulated by IBIS-AS, BATS-FC, IBIS-FC, and BATS-AS

forced using the NNRP2 surrogate climate change scenario and the EH5OM A1B climate change scenario are described below. Presented results are 4.0° × 5.5° spatial averages over the box contained in Fig. 2 unless otherwise noted.

4.1 NCEP-DOE Reanalysis 2 surrogate climate change

Figures 3, 4, and 5 show the difference between the NNRP2 surrogate climate change and NNRP2 control seasonal cycles. 95% confidence intervals were calculated using the Student's t-distribution for both the NNRP2 surrogate climate change and NNRP2 control seasonal cycles. Filled markers in difference figures denote climate change and control confidence intervals that do not overlap. A comparison of the NNRP2 control and observed seasonal cycles is included in the companion paper.

Differences between NNRP2 surrogate climate change and NNRP2 control surface shortwave radiation values are relatively small (Fig. 3). The NNRP2 surrogate climate change seasonal cycles are consistent with the NNRP2 control experiments: IBIS-AS and BATS-AS are generally cloudier and simulate less incident and absorbed surface shortwave radiation during the summer (June–August) than IBIS-FC and BATS-FC. Small differences in the shortwave radiation budget under a surrogate climate change scenario were also found by Seneviratne et al. (2002).

IBIS-AS, BATS-FC, IBIS-FC, and BATS-AS simulate warmer two-meter air temperatures throughout the year when forced using the NNRP2 surrogate climate change boundary conditions instead of the NNRP2 control boundary conditions (Fig. 3). While the NNRP2 control seasonal cycle of two-meter air temperature is a function of both the surface physics scheme and convective closure, warming under the NNRP2 surrogate climate change scenario is controlled largely by convective closure. On average, IBIS-FC and BATS-FC simulate a 3.3°C warming over the summer months, while IBIS-AS and BATS-AS only increase two-meter air temperature 2.1°C. This is in part a function of the reduced cloudiness and increased incident surface shortwave radiation simulated when using the FC80 closure assumption.

Downward longwave radiation is enhanced in all simulations, a result of increasing the concentration of CO_2 equivalent from 355 to 710 ppm, additional water vapor in the atmosphere, and reduced cloudiness in IBIS-FC and BATS-FC during the summer (Fig. 3). The differences between the NNRP2 surrogate climate change net longwave radiation (defined as positive upward) seasonal cycles and the NNRP2 control net longwave radiation seasonal cycles are a function of ground temperature and downward longwave radiation. The increase in downward longwave radiation reduces net longwave radiation, while warmer surface temperatures increase net longwave radiation. Across all models, changes in net longwave radiation are small relative to the interannual variability of the NNRP2 surrogate climate change and NNRP2 control seasonal cycles. The response of two-meter air temperature and downward longwave radiation are approximately consistent with Seneviratne et al. (2002); however, there are differences across model configurations.

Assessing the response of precipitation to the NNRP2 surrogate climate change scenario is difficult given the high interannual variability of precipitation, as described in the companion paper. For all months and model configurations, the 95% confidence intervals of the NNRP2 surrogate climate change and NNRP2 control seasonal cycles overlap. However, annually averaged all models do simulate increased precipitation under the NNRP2 surrogate climate change scenario (Fig. 4). BATS-FC enhances precipitation by 0.8 mm d^{-1} during June–August. The summer precipitation increases in IBIS-AS and BATS-AS are 0.3 and 0.2 mm d^{-1}, respectively. This is consistent with the tendency of the AS74 convective closure assumption to produce more clouds and less variable precipitation in the NNRP2 control simulations. IBIS-AS, BATS-FC, IBIS-FC, and BATS-AS simulate increased evapotranspiration in the early spring (February, March, April), but during the summer changes in evapotranspiration are relatively small, as shown in Fig. 4. The response of precipitation and evapotranspiration to the NNRP2 surrogate climate change scenario is similar to that found by Seneviratne et al. (2002), with some differences resulting from choice of model configuration and years simulated.

Averaged over the summer, the increase in precipitation under the NNRP2 surrogate climate change scenario is greater than the coincident increase in evapotranspiration across all models. This excess water is a key difference between the numerical experiments conducted and previous studies that found soil moisture drying. In Manabe et al. (2004) and Wang (2005), summer precipitation is either reduced or slightly enhanced, which, when paired with increased evapotranspiration, results in summer soil moisture drying.

Like precipitation, changes in total runoff, surface runoff, and groundwater runoff resulting from the NNRP2 surrogate climate change scenario are difficult to assess given the high interannual variability of runoff, as described in the companion paper. The differences in total runoff between the NNRP2 surrogate climate change and NNRP2 control simulations of IBIS-AS and BATS-AS are minimal (Fig. 5). Changes in BATS-FC and IBIS-FC total runoff are larger and dominated by increases in surface runoff resulting from additional precipitation, but still small relative to interannual variability. Total runoff is heavily influenced by convective closure assumption through

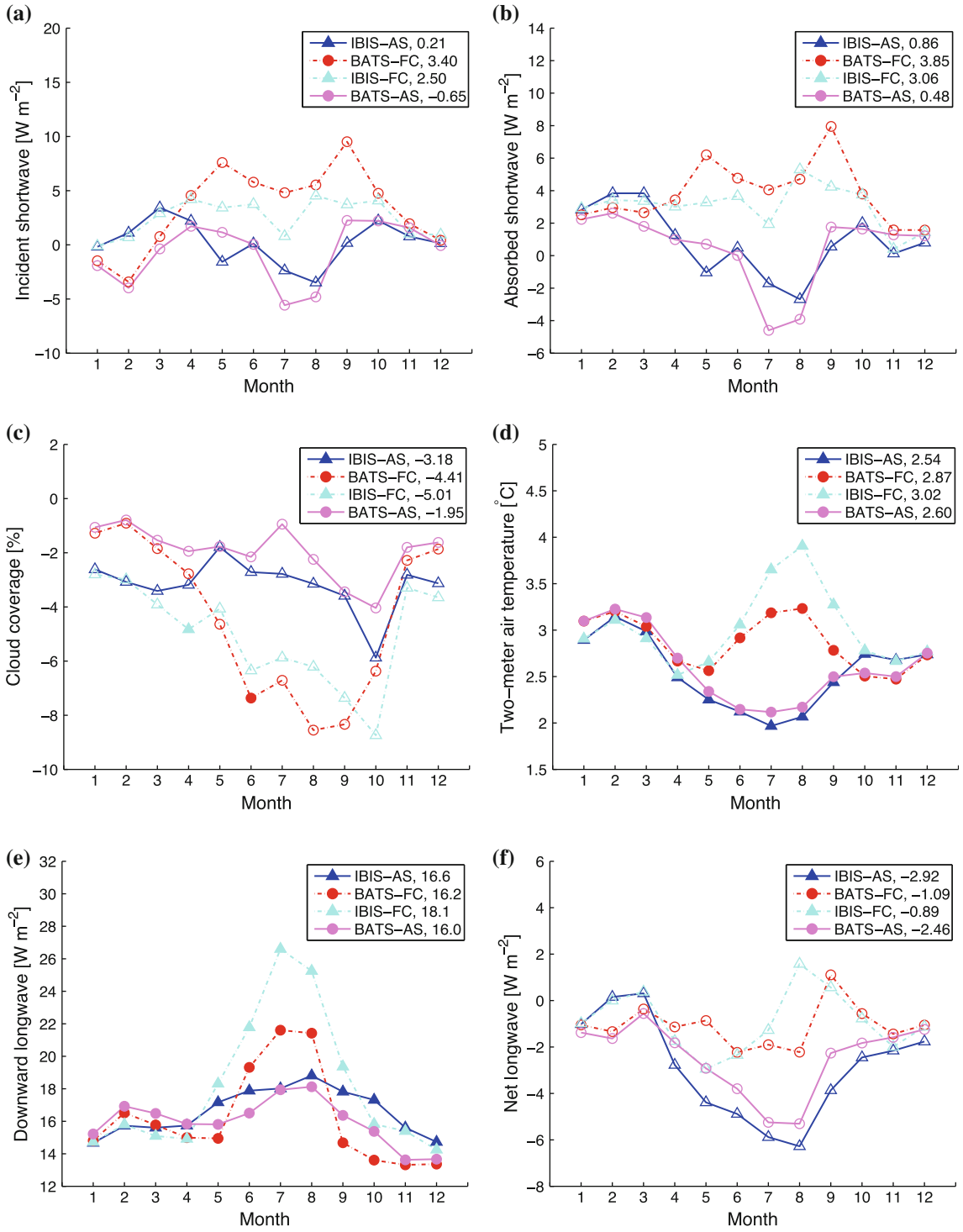

Fig. 3 Difference between NNRP2 surrogate climate change and NNRP2 control seasonal cycles of: **a** incident surface shortwave radiation, **b** absorbed surface shortwave radiation, **c** percentage of maximum model fractional cloud cover (0.8), **d** two-meter air temperature, **e** downward longwave radiation, **f** net longwave radiation (defined as positive upward) for 1984–2004 (two-meter air temperature 1984–2005). *Filled markers* denote non-overlapping confidence intervals in panels (**a**–**f**), and annual averages for each variable examined are provided in the legend

precipitation. The response of total runoff simulated in experiments by Seneviratne et al. (2002) is similar to the response of total runoff simulated by IBIS-AS and BATS-AS. The increase in IBIS-AS and BATS-AS surface runoff is small while the increase in BATS-FC and IBIS-FC surface runoff in the late spring (April–June) and late

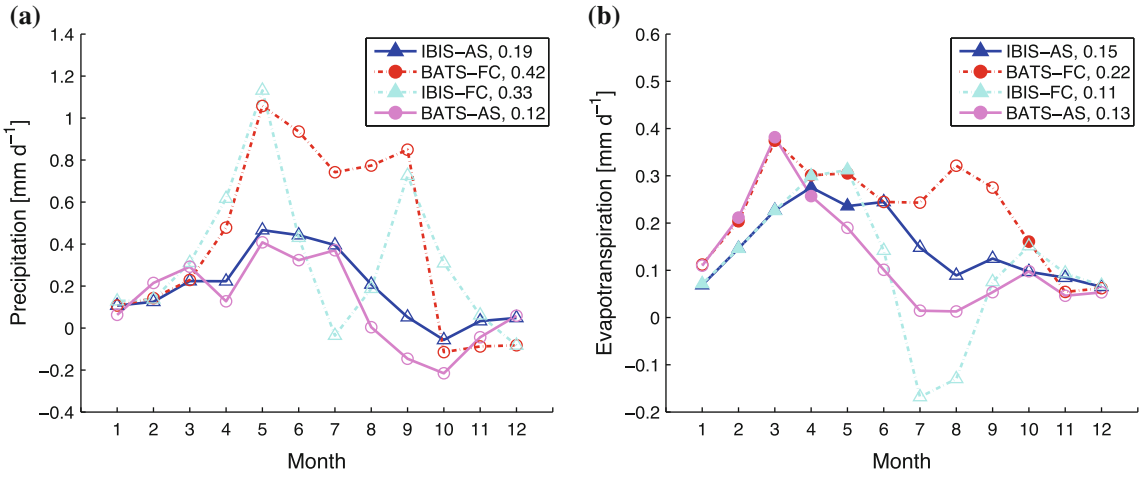

Fig. 4 Difference between NNRP2 surrogate climate change and NNRP2 control seasonal cycles of: **a** precipitation, **b** evapotranspiration for 1984–2005. *Filled markers* denote non-overlapping confidence intervals in panels (**a**, **b**), and annual averages for each variable examined are provided in the legend

summer (July–September) is larger. Changes in groundwater runoff produced by the NNRP2 surrogate climate change forcing are damped when compared with surface runoff. For all months and model configurations, the 95% confidence intervals of the NNRP2 surrogate climate change and NNRP2 control groundwater runoff seasonal cycles overlap.

The differences between the NNRP2 surrogate climate change and NNRP2 control seasonal cycles of surface soil moisture are small throughout the year with the exception of decreased February and March surface soil moisture in IBIS-AS and IBIS-FC and decreased March surface soil moisture in BATS-FC and BATS-AS (Fig. 5). Reductions in surface soil moisture are similar in magnitude to model biases in surface soil moisture, as described in the companion paper. Changes in surface soil moisture under the NNRP2 surrogate climate change scenario are primarily a function of surface physics scheme during the late winter (January–March). The response of root zone soil moisture to the NNRP2 surrogate climate change scenario is negligible. While there is some late summer and early fall (August–October) wetting in BATS-FC, it is trivial compared to the differences in root zone soil moisture across model configurations, as described in the companion paper. This result supports the key finding of this study: there are no substantial summer soil moisture reductions under a warmer climate in the midwestern United States. Minimal changes in soil moisture were also found by Seneviratne et al. (2002) in similar experiments.

Figure 6 shows the differences between the summer (June–August) hydrologic cycles of the NNRP2 surrogate climate change and NNRP2 control simulations throughout the contiguous United States for IBIS-AS and BATS-FC.

Precipitation increases are simulated along the Gulf of Mexico coast by IBIS-AS and the East Coast by BATS-FC. Summer precipitation reductions are found throughout Arizona and western Mexico in IBIS-AS and BATS-FC. The spatial distribution of the summer evapotranspiration response to the NNRP2 surrogate climate change scenario is reasonably well correlated with changes in precipitation; however, the magnitude of the response is damped. IBIS-AS produces increased evapotranspiration in the Gulf of Mexico coast, and BATS-FC produces increased evapotranspiration in the Northeast and through Georgia and South Carolina. Both models simulate decreased evapotranspiration across the southwestern United States and northern Mexico during the summer months, which is primarily a result of reduced precipitation. Enhanced total runoff simulated by BATS-FC is especially prominent over the southeastern United States, and is generated by increased precipitation. Changes in IBIS-AS total runoff during the summer months are relatively small with the exception of the Gulf of Mexico coast, where large increases in June–August precipitation drive enhanced summer total runoff. The differences in summer root zone soil moisture between the NNRP2 surrogate climate change and NNRP2 control simulations of IBIS-AS and BATS-FC are small throughout much of the United States. Soil moisture increases along the Gulf of Mexico coast in IBIS-AS, and to a lesser extent the East Coast in BATS-FC, are a product of enhanced precipitation. Reduced summer root zone soil moisture is simulated by IBIS-AS and BATS-FC over the southwestern United States and northern Mexico. Decreased precipitation, evapotranspiration, and soil moisture in parts of the American Southwest and Mexico, as well as enhanced precipitation in areas of

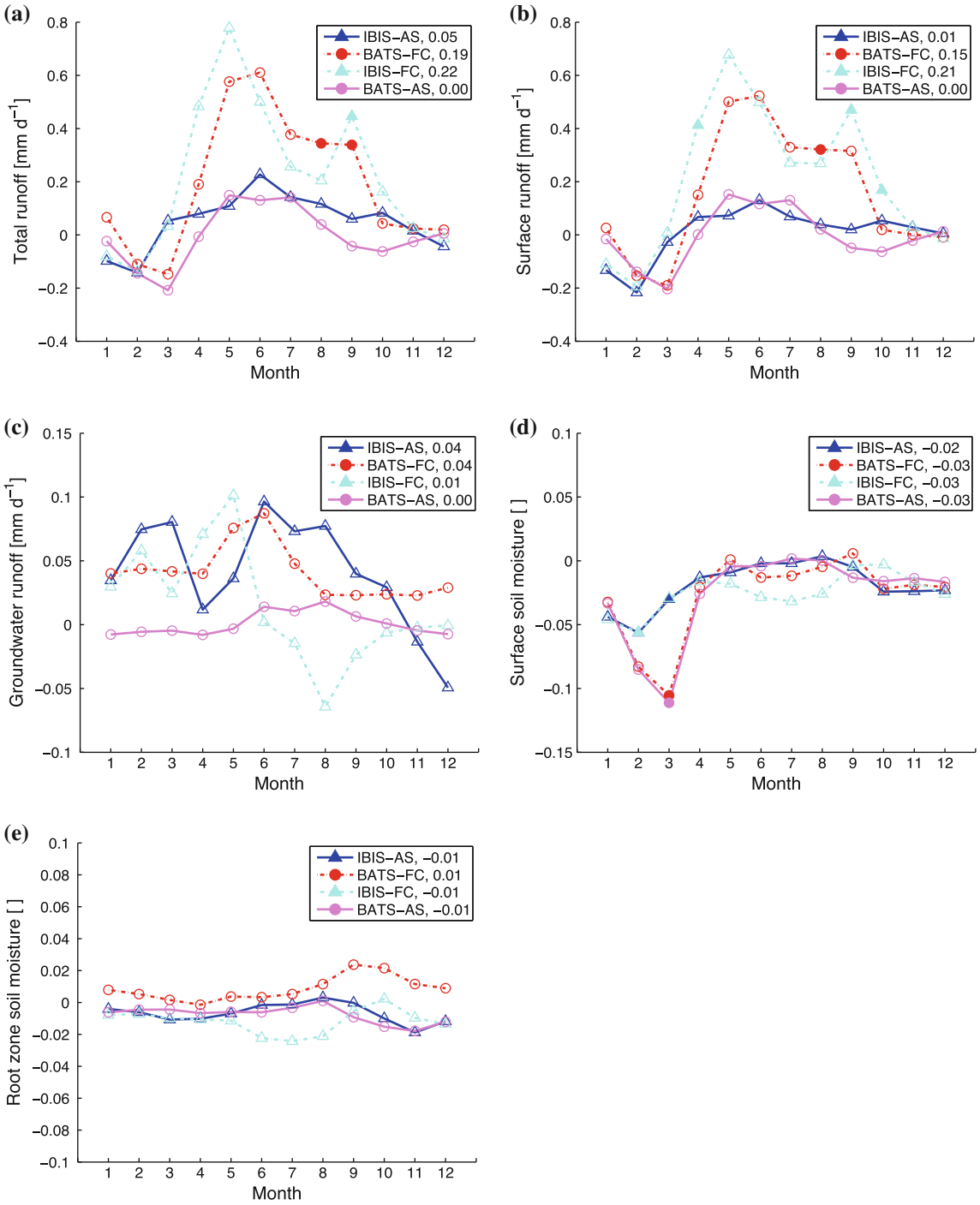

Fig. 5 Difference between NNRP2 surrogate climate change and NNRP2 control seasonal cycles of: **a** total runoff, **b** surface runoff, **c** groundwater runoff, **d** surface soil moisture (0–10 cm), **e** root zone soil moisture (0–100 cm) for 1984–2005 (surface soil moisture and root zone soil moisture 1984–2003). *Filled markers* denote non-overlapping confidence intervals in panels (**a**–**e**), and annual averages for each variable examined are provided in the legend

the southeastern United States are consistent across the model configurations examined.

While changes in precipitation, evapotranspiration, total runoff, and root zone soil moisture are shown for the contiguous United States in Fig. 6, the significance of these changes is difficult to evaluate as the ability of RegCM3 to reproduce the current hydroclimatology was thoroughly assessed over the American Midwest only. Observations of

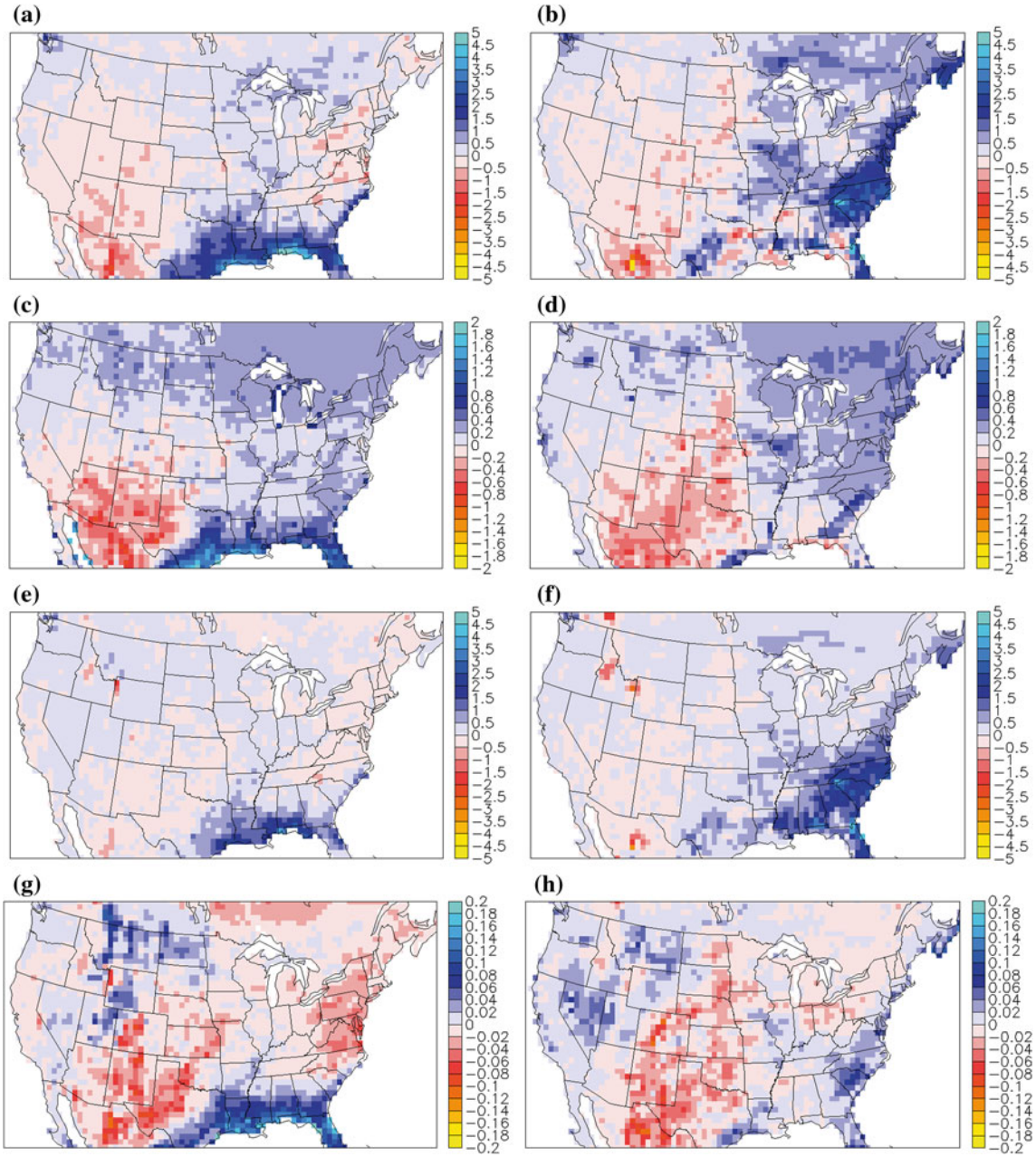

Fig. 6 Difference between NNRP2 surrogate climate change and NNRP2 control simulations of summer (June–August): **a** IBIS-AS precipitation (mm d^{-1}), **b** BATS-FC precipitation (mm d^{-1}), **c** IBIS-AS evapotranspiration (mm d^{-1}), **d** BATS-FC evapotranspiration (mm d^{-1}), **e** IBIS-AS total runoff (mm d^{-1}), **f** BATS-FC total runoff (mm d^{-1}), **g** IBIS-AS root zone soil moisture (0–100 cm, unitless), **h** BATS-FC root zone soil moisture (0–100 cm, unitless)

critical elements of the hydrologic cycle, particularly soil moisture and evapotranspiration, are not available in all areas of the United States.

4.2 ECHAM5 GCM A1B

One model configuration using IBIS (IBIS-AS) and one model configuration using BATS1e (BATS-FC) were forced with boundary conditions derived from the EH5OM A1B climate change simulation to explore the influence of boundary conditions on energy and water fluxes. Model configurations were chosen based on their ability to reproduce the observed summer averages of key variables, specifically two-meter air temperature, precipitation, evapotranspiration, total runoff, and root zone soil moisture, as described in the companion paper.

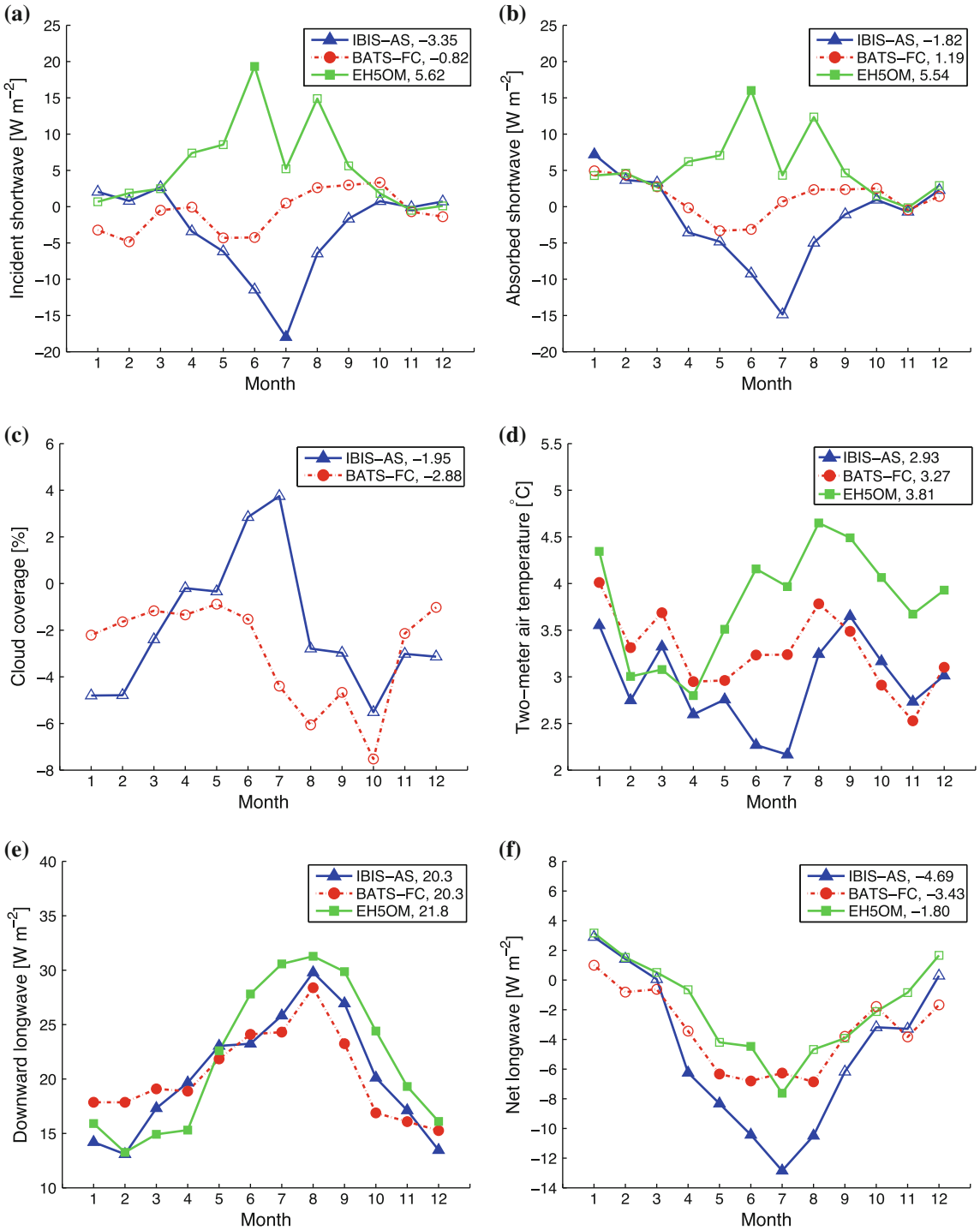

Fig. 7 Difference between EH5OM A1B climate change (2078–2098, two-meter air temperature 2078–2099) and EH5OM control (1984–2004, two-meter air temperature 1984–2005) seasonal cycles of: **a** incident surface shortwave radiation, **b** absorbed surface shortwave radiation, **c** percentage of maximum model fractional cloud cover (0.8), **d** two-meter air temperature, **e** downward longwave radiation, **f** net longwave radiation (defined as positive upward). *Filled markers* denote non-overlapping confidence intervals in panels (**a**–**f**), and annual averages for each variable examined are provided in the legend

Figures 7, 8, and 9 show the difference between the EH5OM A1B climate change and EH5OM control seasonal cycles. 95% confidence intervals were calculated using the Student's t-distribution for both the EH5OM A1B climate change and EH5OM control seasonal cycles. Filled markers in difference figures denote climate change and

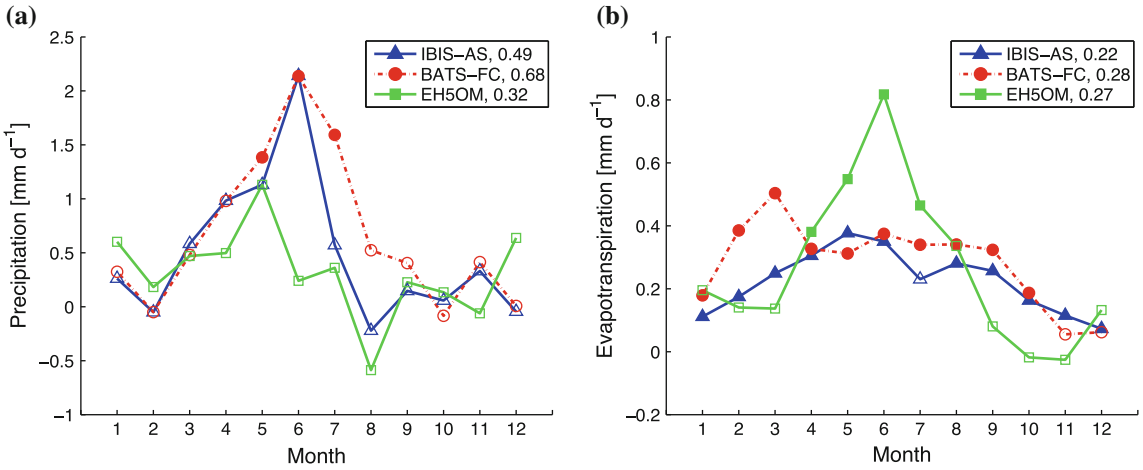

Fig. 8 Difference between EH5OM A1B climate change (2078–2099) and EH5OM control (1984–2005) seasonal cycles of: **a** precipitation, **b** evapotranspiration for 1984–2005. *Filled markers* denote non-overlapping confidence intervals in (**a**, **b**), and annual averages for each variable examined are provided in the legend

control confidence intervals that do not overlap. A comparison of the EH5OM control and observed seasonal cycles is included in the companion paper.

The response of IBIS-AS and BATS-FC incident and absorbed surface shortwave radiation to the EH5OM A1B climate change scenario is shown in Fig. 7. Consistent with the results presented in Sect. 4.1, both models simulate relatively small changes in annually averaged incident and absorbed surface shortwave radiation that are well within model configuration variability. However, IBIS-AS does simulate an 18.0 W m^{-2} reduction in incident surface shortwave radiation during the month of July when forced using EH5OM A1B climate change boundary conditions, a result of increased cloud cover. Future climate (2030–2039) RegCM3 simulations conducted by Diffenbaugh and Ashfaq (2010) show small increases in incident and absorbed surface shortwave radiation.

The EH5OM A1B climate change scenario produces a larger warming than the NNRP2 surrogate climate change scenario annually averaged (Fig. 7). During the summer, the difference between the EH5OM A1B climate change and EH5OM control two-meter air temperature seasonal cycles of IBIS-AS and BATS-FC are 2.6 and 3.4°C, respectively. BATS-FC simulates a larger change in two-meter air temperature, partly a result of reduced cloud cover. Increases in two-meter air temperature produced by the EH5OM A1B climate change scenario seem less dependent on convective closure assumption than increases in two-meter air temperature produced by the NNRP2 surrogate climate change scenario.

The response of downward longwave radiation to the EH5OM A1B climate change forcing is similar in IBIS-AS and BATS-FC, as shown in Fig. 7. This suggests a strong control on downward longwave radiation by boundary conditions. The A1B scenario uses a balance of energy sources (fossil fuel and renewables) to support future growth, with concentrations of CO_2 equivalent varying from 624 ppm in 2076 to 700 ppm in 2100. The slightly larger increases in IBIS-AS and BATS-FC downward longwave radiation under the EH5OM A1B climate change scenario relative to the NNRP2 surrogate climate change scenario are likely a result of disparate atmospheric water vapor and temperatures. The difference between 2030–2039 and 1980–1999 downward longwave radiation found by Diffenbaugh and Ashfaq (2010) is less than that simulated by IBIS-AS and BATS-FC; however, this is expected as 2078–2099 CO_2 equivalent concentrations are higher than 2030–2039 CO_2 equivalent concentrations. IBIS-AS and BATS-FC simulate an 11.3 and 6.6 W m^{-2} reduction in summer net longwave radiation (defined as positive upward), respectively, when forced using EH5OM A1B climate change boundary conditions. The increase in IBIS-AS two-meter air temperature under the EH5OM A1B climate change scenario is smaller than the increase in BATS-FC two-meter air temperature under the EH5OM A1B climate change scenario, which reduces the upward longwave radiation increase and results in a larger net longwave radiation decrease.

The changes to the IBIS-AS and BATS-FC seasonal cycles of precipitation induced by the EH5OM A1B climate change forcing are similar. Both models simulate enhanced precipitation throughout most of the year, with a peak increase of 2.1 mm d^{-1} in IBIS-AS and 2.1 mm d^{-1} in BATS-FC during the month of June. The EH5OM A1B climate change boundary conditions produce a larger response of precipitation in both models than the NNRP2 surrogate climate change boundary conditions annually

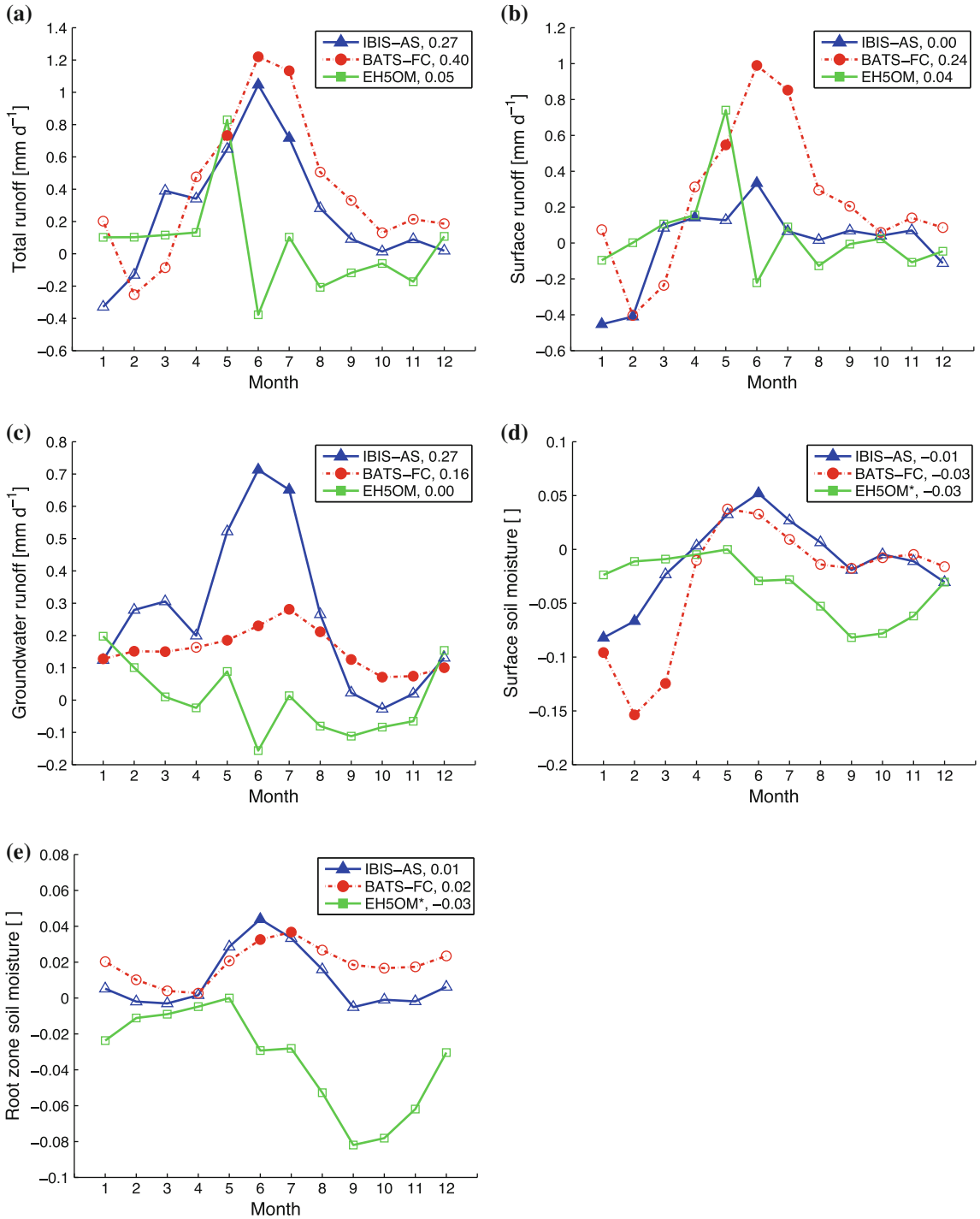

Fig. 9 Difference between EH5OM A1B climate change (2078–2099, surface soil moisture and root zone soil moisture 2078–2097) and EH5OM control (1984–2005, surface soil moisture and root zone soil moisture for 1984–2003) seasonal cycles of: **a** total runoff, **b** surface runoff, **c** groundwater runoff, **d** surface soil moisture (0–10 cm), **e** root zone soil moisture (0–100 cm). *Filled markers* denote non-overlapping confidence intervals in (**a**–**e**), and annual averages for each variable examined are provided in the legend

averaged. IBIS-AS and BATS-FC simulate increased evapotranspiration for most months under the EH5OM A1B climate change scenario, with the exception of July in IBIS-AS and November and December in BATS-FC. As with precipitation, the response of evapotranspiration in both models is larger when forced using the EH5OM A1B

climate change boundary conditions instead of NNRP2 surrogate climate change boundary conditions.

Consistent with the response of IBIS-AS and BATS-FC to the NNRP2 surrogate climate change scenario, the simulated increase in average summer precipitation under the EH5OM A1B climate change scenario is greater than the coincident increase in average summer evapotranspiration across both models. This excess water is a key difference between the numerical experiments conducted and previous studies that found soil moisture drying. In Manabe et al. (2004) and Wang (2005), summer precipitation is either reduced or slightly enhanced, which, when paired with increased evapotranspiration, results in summer soil moisture drying. Diffenbaugh and Ashfaq (2010) found that 2030–2039 summer precipitation was less than 1980–1999 summer precipitation. The response of the EH5OM model itself, however, is consistent with soil moisture drying, as increases in evapotranspiration are larger than increases in precipitation during the months of June and July.

Large total runoff increases are produced by the EH5OM A1B climate change forcing during the summer (Fig. 9). Averaged over the months of June and July, the amount of total runoff produced increases by 0.9 mm d^{-1} in IBIS-AS and 1.2 mm d^{-1} in BATS-FC, primarily in response to enhanced precipitation. Increases in IBIS-AS and BATS-FC total runoff generated by the EH5OM A1B climate change boundary conditions are larger than increases in IBIS-AS and BATS-FC total runoff resulting from the NNRP2 surrogate climate change boundary conditions annually averaged. Under the EH5OM A1B climate change scenario, BATS-FC simulates a 0.8 mm d^{-1} increase in surface runoff averaged over May–July. The majority of total runoff in BATS-FC occurs as surface runoff. IBIS-AS has a more muted response of surface runoff to the EH5OM A1B climate change forcing than BATS-FC. In both IBIS-AS and BATS-FC, the EH5OM A1B climate change scenario produces a larger response in summer surface runoff than the NNRP2 surrogate climate change scenario. BATS-FC forced using the EH5OM A1B climate change scenario simulates increased groundwater runoff in all months except April; however, groundwater runoff remains a relatively small component of total runoff in BATS-FC. In contrast, the response of groundwater runoff in IBIS-AS to the EH5OM A1B climate change scenario is larger than the response of surface runoff in June and July (0.7 mm d^{-1}).

While surface soil moisture does decrease in January and February under the EH5OM A1B climate change scenario, summer surface soil moisture in IBIS-AS and BATS-FC forced by the EH5OM A1B climate change scenario is equal to or greater than summer surface soil moisture in IBIS-AS and BATS-FC forced by the EH5OM control scenario. Differences between the EH5OM A1B climate change and EH5OM control root zone soil moisture seasonal cycles of IBIS-AS and BATS-FC are positive or negligible, as shown in Fig. 9. Increased precipitation is almost completely compensated for by enhanced evapotranspiration and total runoff. The lack of response in root zone soil moisture to the EH5OM A1B climate change scenario reinforces the key finding of this study: there are no substantial summer soil moisture reductions under a warmer climate in the midwestern United States.

Figure 10 shows the differences between the summer (June–August) hydrologic cycles of the EH5OM A1B climate change (2078-2099) and EH5OM control (1984-2005) simulations for IBIS-AS and BATS-FC throughout the contiguous United States.

The EH5OM A1B climate change scenario enhances IBIS-AS and BATS-FC summer precipitation in parts of the midwestern United States and reduces summer precipitation over the Southwest. BATS-FC simulates large increases in summer precipitation throughout the Southeast and markedly reduced summer precipitation along Mississippi, Louisiana, and southeastern Texas. Differences in precipitation bear little resemblance to the mid-century (2041-2050) changes in precipitation found by Liang et al. (2006). The response of precipitation simulated by IBIS-AS and BATS-FC also differs from 2030–2039 mean changes found by Diffenbaugh and Ashfaq (2010), which include extensive drying across the midwestern United States. Changes in summer evapotranspiration are relatively small in both IBIS-AS and BATS-FC forced using the EH5OM A1B climate change boundary conditions, with modest increases across much of the United States with the exception of the American Southwest. The response of summer total runoff produced by the EH5OM A1B climate change scenario is well correlated with the reponse of precipitation. IBIS-AS simulates increased total runoff over the midwestern and central United States and decreased total runoff over the southwestern United States. BATS-FC simulates increased total runoff across the American Midwest and Southeast and decreased summer total runoff throughout Mississippi, Louisiana, and southeastern Texas. IBIS-AS and BATS-FC forced using the EH5OM A1B climate change scenario contain more pronounced reductions in summer root zone soil moisture over the Southwest than IBIS-AS and BATS-FC forced using the NNRP2 surrogate climate change scenario. BATS-FC also simulates reduced summer root zone soil moisture along southern Louisiana and southeastern Texas under the EH5OM A1B climate change scenario. Diffenbaugh and Ashfaq (2010) found decreases in average soil moisture in 2030–2039 across the American Midwest, which does not agree with the unchanged or slightly increased root zone soil moisture found in this set of numerical experiments. Decreased

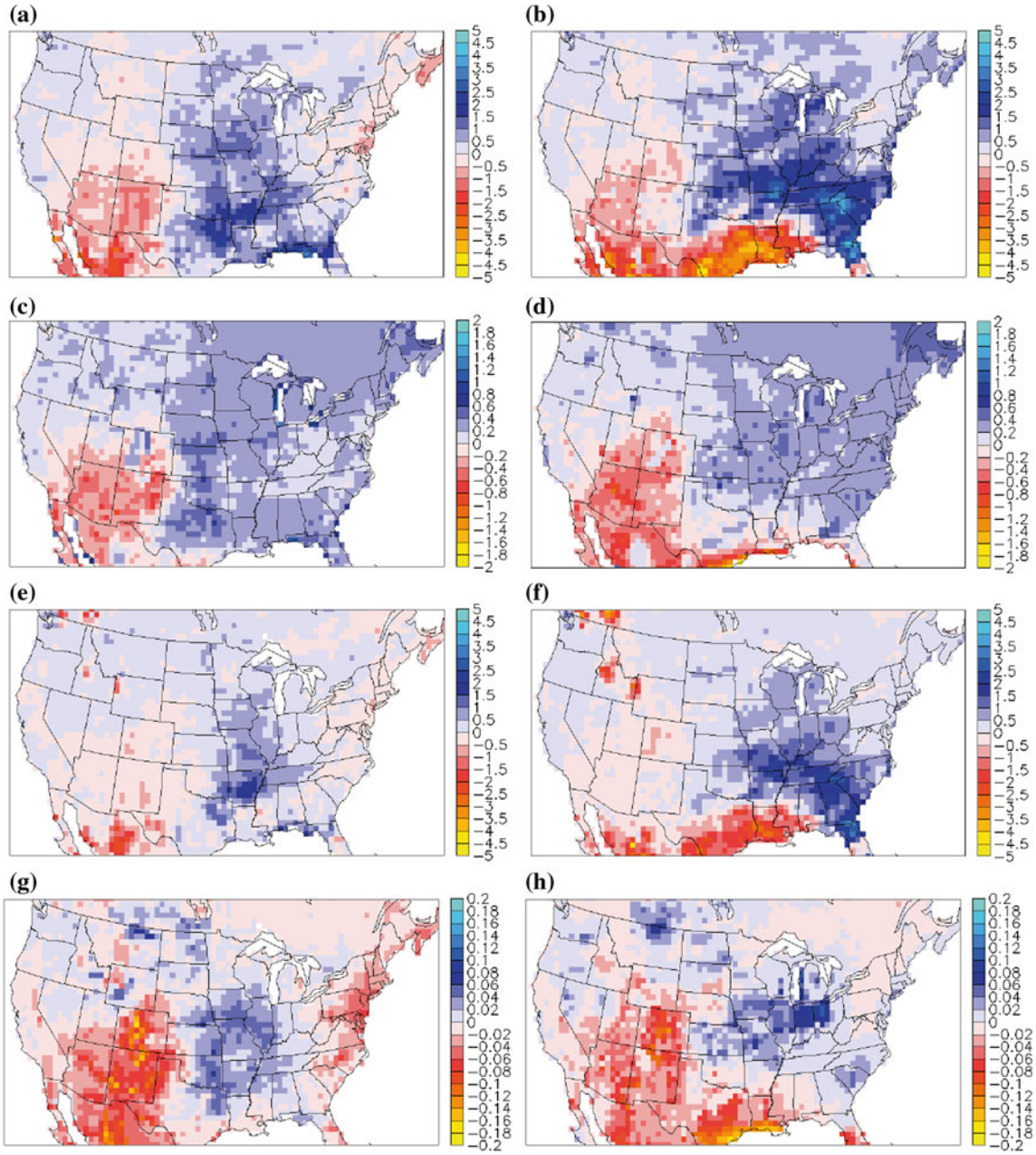

Fig. 10 Difference between EH5OM A1B climate change (2078–2099) and EH5OM control (1984–2005) simulations of summer (June–August): **a** IBIS-AS precipitation (mm d^{-1}), **b** BATS-FC precipitation (mm d^{-1}), **c** IBIS-AS evapotranspiration (mm d^{-1}), **d** BATS-FC evapotranspiration (mm d^{-1}), **e** IBIS-AS total runoff (mm d^{-1}), **f** BATS-FC total runoff (mm d^{-1}), **g** IBIS-AS root zone soil moisture (0–100 cm, unitless), **h** BATS-FC root zone soil moisture (0–100 cm, unitless)

precipitation, evapotranspiration, and soil moisture in parts of the American Southwest and Mexico, as well as enhanced precipitation over the midwestern United States are consistent across the model configurations examined.

While changes in precipitation, evapotranspiration, total runoff, and root zone soil moisture are shown for the contiguous United States in Fig. 10, the significance of these changes is difficult to evaluate as the ability of RegCM3 to reproduce the current hydroclimatology was thoroughly assessed over the American Midwest only. Observations of critical elements of the hydrologic cycle, particularly soil moisture and evapotranspiration, are not available in all areas of the United States.

Figure 11 shows the mean NNRP2 control, NNRP2 surrogate climate change, EH5OM control, and EH5OM A1B climate change seasonal cycles for key hydrologic variables. Each seasonal cycle includes error bars showing 95% confidence intervals calculated using the

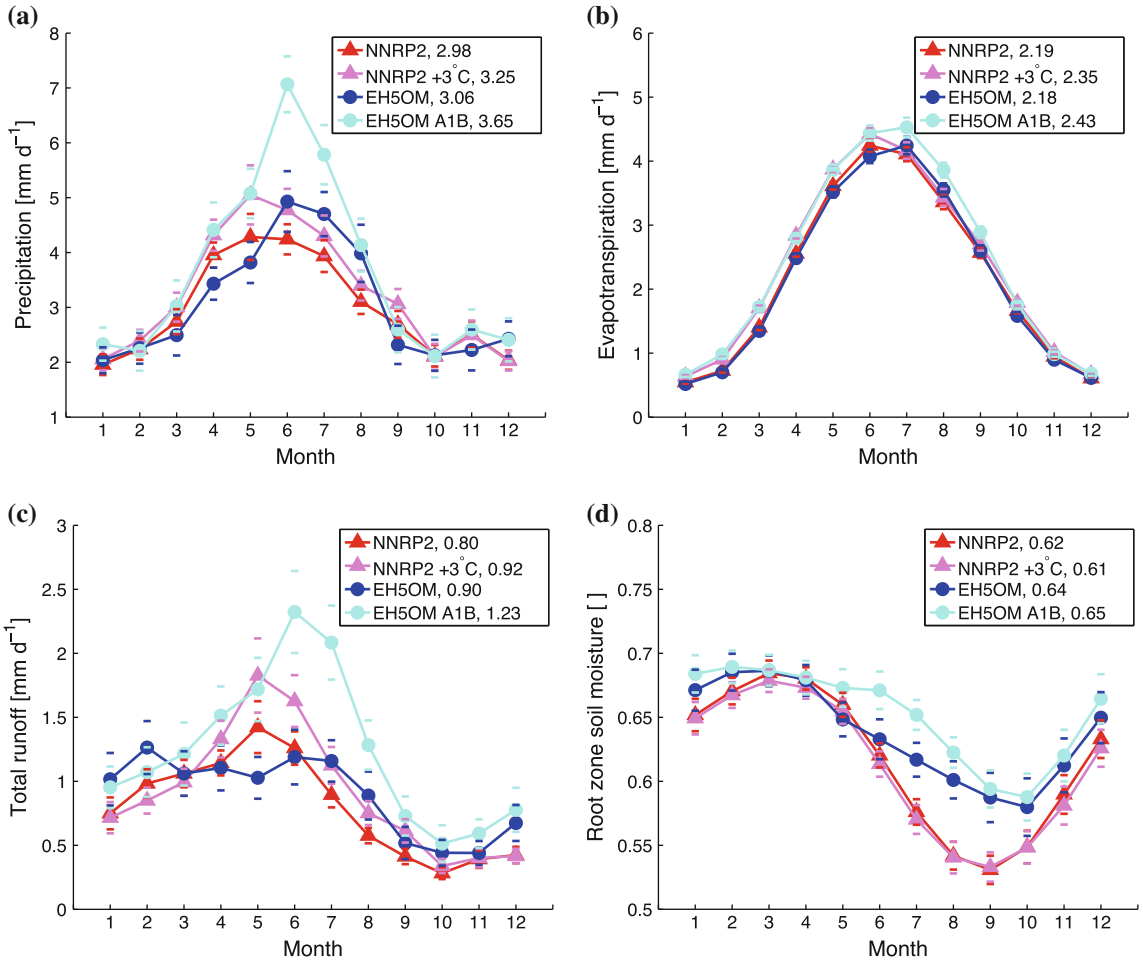

Fig. 11 Mean seasonal cycles of: **a** precipitation, **b** evapotranspiration, **c** total runoff, **d** root zone soil moisture (0–100 cm) for NNRP2 control (1984–2005, root zone soil moisture 1984–2003), NNRP2 surrogate climate change (1984–2005, root zone soil moisture 1984–2003), EH5OM control (1984–2005, root zone soil moisture 1984–2003), and EH5OM A1B climate change (2078–2099, root zone soil moisture 2078–2097). *Error bars* showing 95% confidence intervals are included in (**a**–**d**), and annual averages for each variable examined are provided in the legend

Student's t-distribution. During the months of April through July, EH5OM A1B climate change precipitation is larger than EH5OM control precipitation. Large interannual variability in precipitation makes model evaluation difficult, and disregarding error bars both the NNRP2 surrogate and EH5OM A1B climate change scenarios simulate more spring and summer precipitation than the NNRP2 and EH5OM control scenarios, respectively. Evapotranspiration is enhanced during the winter (December–February) and spring in the NNRP2 surrogate climate change simulations, and throughout most of the year (January–October) in the EH5OM A1B climate change simulations. Total runoff simulated by models forced using the NNRP2 surrogate climate change scenario is greater than total runoff simulated by models forced using the NNRP2 control scenario in June, August, and September, and total runoff simulated by models forced using the EH5OM A1B climate change scenario is greater than total runoff simulated by models forced using the EH5OM control scenario in April through August. Consistent with the results presented above, no decreases in root zone soil moisture are found between either the NNRP2 surrogate climate change and NNRP2 control or EH5OM A1B climate change and EH5OM control experiments.

5 Summary and conclusions

The American Midwest is a critical agricultural region with an extensive observational record that includes major components of the hydrologic cycle. This makes the midwestern United States an ideal location for evaluating the impacts of climate change on croplands. After throughly assessing the ability of RegCM3-IBIS and RegCM3-BATS1e to simulate the hydroclimatology of the American

Midwest in the companion paper, the response of RegCM3-IBIS and RegCM3-BATS1e to climate change was explored. Two sets of experiments were conducted to evaluate this response. First, the surrogate climate change scenario of Schär et al. (1996) was used. Realistic boundary conditions (NNRP2) were warmed by 3°C with a corresponding increase in the concentration of CO_2 equivalent. Second, the boundaries of RegCM3-IBIS and RegCM3-BATS1e were forced using output from the ECHAM5 GCM run under the A1B emissions scenario with a corresponding increase in the concentration of CO_2 equivalent.

Qualitatively, both climate change experiments produced similar results. Several findings are robust across boundary conditions, surface physics schemes, and convective closure assumptions. These findings include: warmer two-meter air temperatures, increased downward longwave radiation, increased spring evapotranspiration, and unchanged or increased root zone soil moisture. All experiments also contain increases in summer precipitation, total runoff, surface runoff, and groundwater runoff; however, the significance of the differences between climate change and control scenarios is difficult to evaluate given the high interannual variability of precipitation and runoff, as shown in the companion paper.

The response of the shortwave radiation budget to both climate change scenarios is relatively small in the simulations examined, and is most dependent on convective closure assumption and boundary conditions. Differences between climate change and control longwave radiation, two-meter air temperature, and precipitation are influenced by boundary conditions, convective closure, and in some cases surface physics scheme. Changes in evapotranspiration during the spring are largely a function of surface physics scheme and boundary conditions, and changes in evapotranspiration throughout the summer can be dependent on convective closure. Differences between climate change and control total runoff are heavily influenced by convective closure assumption and boundary conditions, while differences between climate change and control groundwater runoff, surface soil moisture, and root zone soil moisture are more dependent on surface physics scheme and boundary conditions. The response of IBIS-AS and BATS-FC seasonal cycles to the EH5OM A1B forcing is similar across a number of variables, including two-meter air temperature, precipitation, evapotranspiration, total runoff, surface soil moisture, and root zone soil moisture. This suggests that large-scale processes play a substantial role determining the response of the hydrologic cycle to future climate and that IBIS-AS and BATS-FC respond similarly for some variables, which is expected as both models were chosen because of their ability to reproduce the current climate.

One of the largest potential impacts of climate change is the drying of soils over agriculturally productive areas, such as the midwestern United States. The fundamental conclusion of these experiments is that there are no reductions in summer surface or root zone soil moisture under either of the climate change scenarios examined. While higher temperatures and increased downward longwave radiation do result in enhanced evapotranspiration, the coincident increase in precipitation more than balances the larger fluxes of latent heat, and ultimately results in additional surface and groundwater runoff.

Acknowledgments We thank the International Centre for Theoretical Physics, the Eltahir group, members of the Ralph M. Parsons Laboratory who aided in this research, our reviewers, and our editor. Individuals who made significant contributions to this work include Jeremy Pal and Marc Marcella. This work was funded by the National Science Foundation (Award EAR-04500341) and the Martin Family Fellowship.

References

Arakawa A, Schubert WH (1974) Interaction of a cumulus cloud ensemble with large-scale environment, Part 1. J Atmos Sci 31:674–701

Dickinson R, Henderson-Sellers A, Kennedy P (1993) Biosphere atmosphere transfer scheme (BATS) version 1E as coupled to the NCAR community climate model. Technical Note TN-387+STR, National Center for Atmospheric Research

Diffenbaugh NS, Ashfaq M (2010) Intensification of hot extremes in the united states. Geophys Res Lett 37:L15,701

Foley JA, Prentice IC, Ramankutty N, Levis S, Pollard D, Sitch S, Haxeltine A (1996) An integrated biosphere model of land surface processes, terrestrial carbon balance, and vegetation dynamics. Global Biogeochem Cycles 10:603–628

Fritsch JM, Chappell CF (1980) Numerical prediction of convectively driven mesoscale pressure systems part I: convective parameterizations. J Atmos Sci 37:1722–1733

Grell GA, Dudhia J, Stauffer D (1994) A description of the fifth-generation Penn State/NCAR mesoscale model (MM5). Technical Note TN-398+IA, National Center for Atmospheric Research

Harrison P, Bruinsma J, de Haen H, Alexandratos N, Schmidhuber J, Bödeker G, Ottaviani MG (2002) World agriculture: towards 2015/2030. Online, http://www.fao.org/documents/

Karl TR, Melillo JM, Peterson TC (eds) (2009) Global climate change impacts in the United States. Cambridge University Press, Cambridge

Liang XZ, Pan J, Zhu J, Kunkel KE, Wang JXL, Dai A (2006) Regional climate model downscaling of the U.S. summer climate and future change. J Geophys Res 111:D10,108

Manabe S, Wetherald RT (2002) Simulation of hydrologic changes associated with global warming. J Geophys Res 107:4379

Manabe S, Weatherald RT, Stouffer RJ (1981) Summer dryness due to an increase of atmospheric CO_2 concentration. Clim Change 3:347–386

Manabe S, Wetherald RT, Milly PCD, Delworth TL, Stouffer RJ (2004) Century-scale changes in water availability: CO_2 quadrupling experiment. Clim Change 64:59–76

Meehl GA, Washington WM (1988) A comparison of soil-moisture sensitivity in two global climate models. J Atmos Sci 45:1476–1492

Nakicenovic N, Alcamo J, Davis G, de Vries B, Fenhann J, Gaffin S, Gregory K, Grübler A, Jung TY, Kram T, La Rovere EL, Michaelis L, Mori S, Morita T, Pepper W, Pitcher H, Price L, Raihi K, Roehrl A, Rogner HH, Sankovski A, Schlesinger M, Shukla P, Smith S, Swart R, van Rooijen S, Victor N, Dadi Z (2000) IPCC special report on emissions scenarios. Cambridge University Press, Cambridge

Pal JS, Giorgi F, Bi X, Elguindi N, Solmon F, Gao X, Rauscher SA, Francisco R, Zakey A, Winter J, Ashfaq M, Syed FS, Bell JL, Diffenbaugh NS, Karmacharya J, Konaré A, Martinez D, Da Rocha RP, Sloan LC, Steiner AL (2007) Regional climate modeling for the developing world: the ICTP RegCM3 and RegCNET. Bull Am Meteorol Soc 88:1395–1409

Ramankutty N (1999) Estimating historical changes in land cover: North American croplands from 1850 to 1992. Global Ecol Biogeogr 8:381–396

Randall DA, Wood RA, Bony S, Colman R, Fichefet T, Fyfe J, Kattsov V, Pitman A, Shukla J, Srinivasan J, Stouffer RJ, Sumi A, Taylor KE (2007) Climate models and their evaluation. In: Climate change 2007: the physical science basis. Contribution of working group I to the fourth assessment report of the intergovernmental panel on climate change. Cambridge University Press, Cambridge

Rosenzweig C, Iglesias A, Yang XB, Epstein PR, Chivian E (2001) Climate change and extreme weather events: implications for food production, plant diseases, and pests. Global Change Human Health 2:90–104

Schär C, Frei C, Lüthi D, Davies H (1996) Surrogate climate-change scenarios for regional climate models. Geophys Res Lett 23:669–672

Seneviratne SI, Pal JS, Eltahir EAB, Schär C (2002) Summer dryness in a warmer climate: a process study with a regional climate model. Clim Dyn 20:69–85

USGS (1996) Global 30-Arc Second elevation dataset (GTOPO30). Online, http://edc.usgs.gov/products/elevation/gtopo30/gtopo30.html

Wang G (2005) Agricultural drought in a future climate: results from 15 global climate models participating the the 4th assessment. Clim Dyn 25:739–753

Winter JM, Pal JS, Eltahir EAB (2009) Coupling of integrated biosphere simulator to regional climate model version 3. J Clim 22:2743–2757

Wuebbles DJ, Hayhoe K (2004) Climate chance projections for the United States midwest. Mitig Adapt Strat Global Change 9:335–363